Effect of Compton scattering on the double-to-single photoionization ratio in helium

M. Sagurton,[1] R. J. Bartlett,[2] J. A. R. Samson,[3] Z. X. He,[3] and D. Morgan[2]
[1]*SFA, Inc., 1401 McCormick Drive, Landover, Maryland 20785*
[2]*Los Alamos National Laboratory, Los Alamos, New Mexico 87545*
[3]*Department of Physics and Astronomy, University of Nebraska, Lincoln, Nebraska 68588-0111*
(Received 23 March 1995)

The effect of Compton scattering on the ratio of double-to-single ionization from photon impact in helium has been measured for $2.1 \leq h\nu \leq 5.5$ keV using a time-of-flight ion spectrometer with a high relative collection efficiency for Compton ions. Single ionization from Compton scattering is found to contribute measurably to a reduction in the ionization ratio for $h\nu \gtrsim 3.5$ keV. Our measurements are compared with predictions based on recent calculations of the single and double ionization cross sections for photoabsorption and Compton scattering by Hino *et al.* [Phys. Rev. A **48**, 1271 (1993), Phys. Rev. Lett. **72**, 1620 (1994)], Andersson *et al.* [Phys. Rev. Lett. **71**, 50 (1993)], and Surić *et al.* [Phys. Rev. Lett. **73**, 790 (1994)].

PACS number(s): 32.80.Cy, 32.80.Fb

It is well known that double ionization from photon impact in many-electron atoms is a direct consequence of electron correlation in the initial and final states. Indeed, the matrix element for double ionization vanishes if taken between one-electron wave functions, because the interaction Hamiltonian is a one-body operator [1]. Double ionization, therefore, provides an excellent tool for studying electron correlation in atoms. Helium, as the simplest many-electron neutral atom, has served as a test case. In the high $h\nu$ regime theoretical interest initially focused on the $h\nu \rightarrow \infty$ (but nonrelativistic) limit of the ratio $R_p(h\nu) = \sigma_p^{2+}(h\nu)/\sigma_p^{+}(h\nu)$ of the double- and single-ionization cross sections in photoabsorption, because the description of electron correlation in this limit simplifies considerably. While early studies [2–5] gave varying results for $R_p(\infty)$ ranging from 1.6% to 2.3%, recent work [6,7] appears to establish that $R_p(\infty) = 1.66\%$. Of particular significance, it has also been demonstrated [6,7] that $R_p(\infty)$ is independent of final-state correlation, implying that an experimental determination of $R_p(\infty)$ would provide an independent test of the theoretical description of ground-state correlation. With advances in computational methods, the calculation of $R_p(h\nu)$ has recently been extended down to the soft-x-ray regime above 1 keV [7–9] where final-state correlation becomes important. Here, however, there is some uncertainty regarding the correct value of σ_p^{2+}. For example, for $h\nu = 2.0$ keV Hino *et al.* [9] obtain $R_p = 1.82\%$ using many-body perturbation theory (MBPT), while Andersson and Burgdörfer [7] obtain $R_p = 2.53\%$ and 2.10% using different approximations for the final-state wave function at intermediate energies.

To date, to our knowledge the only experiments on He for $h\nu > 1$ keV have been by Levin *et al.* [10,11], who measured the double-to-single ionization ratio $R(h\nu)$ for $2.05 \leq h\nu \leq 4.0$ keV, near $h\nu = 8.5$ keV, and near $h\nu = 11.5$ keV, where R_p is expected to be within a few percent of $R_p(\infty)$. These measurements were initially interpreted as being consistent with a value for $R_p(\infty)$ of $1.5\% \pm 0.2\%$ [11]. However, Samson, Greene, and Bartlett [12] emphasized that Compton scattering will become the dominant process for single ionization in He for $h\nu \gtrsim 7$ keV, where the increasing cross section for Compton ionization crosses over with the steeply decreasing [as $\approx (h\nu)^{-3.5}$] photoabsorption cross section. Thus, at the higher $h\nu$ Levin *et al.*'s measurements reflect primarily the Compton ionization processes, and the experimental value of $R_p(\infty)$ remains undetermined. Compton ionization has now been measured directly in He for $3.0 \leq h\nu \leq 5.5$ keV [13].

Very recently, efforts have been undertaken [7,14–17] to calculate the ratio $R_C = \sigma_C^{2+}/\sigma_C^{+}$ of the double- and single-ionization cross sections for Compton scattering from He. In the soft-x-ray region, approximations for single ionization which become valid at very high $h\nu$, such as the impulse approximation [18,19] (IA), are not expected to be adequate. Also, as in the case of photoabsorption, electron correlation must be incorporated to describe double ionization; however in Compton ionization both final-state electrons generally leave with low kinetic energy for $h\nu$ within several keV of threshold. In the high $h\nu$ limit, Surić *et al.* [14] obtained $R_C(\infty) = 0.80\%$ with the nonrelativistic impulse approximation, while Andersson and Burgdörfer [15] obtained $R_C(\infty) = 0.84\%$ in calculations employing a fully correlated ground state and approximate correlated final states. However, for the intermediate photon energy of 12 keV Surić *et al.* obtained $R_C = 0.66\%$, while Andersson and Burgdörfer obtained values ranging from 1.06% to 1.29%, depending on the final-state approximation [7,15]. Hino, Bergstrom, and Macek [16] calculated R_C for $4 \leq h\nu \leq 12$ keV, using MBPT to evaluate the A^2 term in the interaction Hamiltonian to first order, and obtained $R_C = 1.67\%$ for $h\nu = 12$ keV. In contrast with their initial assumption, however, more recent work by these authors [17] indicates that their calculation has not approached its asymptotic limit by $h\nu = 12$ keV. Thus, at least for lower photon energies, there are large disagreements among the existing calculations of R_C. Furthermore, unlike the situation in the case of photoabsorption, these disagreements involve the cross sections for both double *and* single ionization.

In this paper we report measurements of the double-to-single photoionization ratio for He for $2.1 \leq h\nu \leq 5.5$ keV,

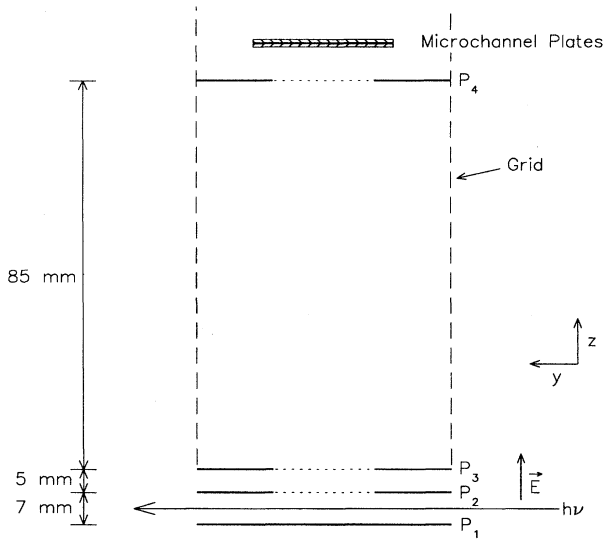

FIG. 1. Time-of-flight ion spectrometer.

obtained with a time-of-flight spectrometer (TOFS) with a substantially higher collection efficiency for Compton ions than for ions created through photoabsorption. [We shall denote the ionization ratio that incorporates the spectrometer collection efficiencies as $R_m(h\nu)$ to distinguish it from the ratio $R(h\nu)$ of the total double- and single-ionization cross sections.] For $4<h\nu\leq 5.5$ keV the deviation of $R(h\nu)$ from $R_p(h\nu)$ due to Compton ionization is shown to become substantial. Our experimental results are compared with predicted values for $R_m(h\nu)$ obtained by weighting the cross sections of Andersson and Burgdörfer [7], Hino *et al.* [9,16], and Surić *et al.* [14] with the appropriate experimental collection efficiencies.

The experiments were performed on the Los Alamos National Laboratory soft x-ray beamline X8A at the National Synchrotron Light Source. $h\nu=2.1$ keV is the lowest photon energy accessible with the Si(111) monochromator crystals. Above $h\nu=5.5$ keV the reflectivity falloff of the Ni-coated beamline focusing mirror (incidence angle $=10$ mrad, nominal energy cutoff $=5.9$ keV) results in an unacceptably small count rate. The beam profile in the end station was ≈ 4 mm (horizontal)$\times 2$ mm (vertical). uv light specularly reflected from the monochromator crystals was eliminated with a 0.5 μm Ni filter (transmission at 100 eV is 4.2×10^{-12}). Helium was introduced into the sample chamber from an effusive gas nozzle located ≈ 15 mm from the beam path, and an ambient pressure of 2.8×10^{-6} torr was maintained with a feedback controlled valve. Separate count rates for He^+ and He^{2+} ions were measured with a time-of-flight spectrometer, illustrated in Fig. 1. The x-ray beam was polarized parallel to the TOFS axis.

The x-ray beam path lies in an ion "extraction" region between TOFS plates P_1 and P_2. Plates P_2 and P_3 define an "acceleration" region, and plates P_3 and P_4 a field free drift region. Voltage pulses of magnitude V_1, V_2 applied to P_1, P_2, respectively, generate a field parallel to the spectrometer axis which extracts and accelerates the ions which accumulate in the extraction region before the field pulse arrives. P_3 and P_4 are held at ground. For the present measurements V_1 and V_2 were 700 and 500 V, respectively, the pulse period T was 8 μs (in a few cases 9 μs), and the pulse width was 200 ns. The detector consists of dual microchannel plates (MCP's) biased at -5.46 kV to ensure equal detection efficiencies for the single- and double-ionization states [10]. 19 mm diameter (mesh covered) holes in plates P_2–P_4 allow ions to pass through to the detector. The voltage pulse rise provides the start pulse and the signal from the MCP's the stop pulse in a time-to-pulse-height converter. Mean flight times for the He^+ and He^{2+} ions were ≈ 667 and 472 ns, respectively. The count rates for He^+ and He^{2+} varied from ≈ 0.65 counts/s and 0.012 counts/s, respectively, for $h\nu=2.1$ keV, to ≈ 0.11 counts/s and 0.0013 counts/s, respectively, for $h\nu=5.5$ keV.

To prevent electron-impact ionization from contributing to the He^+, He^{2+} signals, electrons must be excluded from the extraction region. Successive upstream aperturing of the x-ray beam eliminated the generation of photoelectrons from plates P_1 and P_2. Magnets placed along the beam pipe upstream and downstream of the spectrometer chamber rejected externally generated electrons.

Because the He^+ and He^{2+} ions which accumulate in the extraction region have nonzero velocities, due both to their thermal motion and to the recoil induced during ionization, a certain percentage will drift out of the extraction-acceleration region before the field pulse arrives or strike one of the TOFS plates P_1–P_4 either before the field pulse arrives or while traveling to the detector. The collection efficiency of the TOFS is therefore less than 1. An additional complication is that a certain percentage of the ions which drift into the acceleration region before the field pulse arrives, or which are created while the field is on, will fail to receive the full impulse from the field and so arrive at the detector late.

Let η_p^+ and η_C^+ denote the collection efficiencies for He^+ ions created through photoabsorption and Compton scattering, respectively, and let η_p^{2+} and η_C^{2+} denote the corresponding collection efficiencies for He^{2+} ions. η_p^{2+} is slightly greater than η_p^+ (and similarly for η_C^{2+} and η_C^+) because the time of flight is shorter for He^{2+} ions and thus fewer are lost to drift perpendicular to the TOFS axis. However, η_p^+ is considerably smaller than η_C^+ due to the large ion recoil velocity v_R in photoabsorption. Neglecting the photon momentum,

$$v_R=0.08129(h\nu-24.59)^{1/2}\ \text{mm}/\mu\text{s} \qquad (1)$$

for $h\nu$ in eV, where 24.59 eV is the He($1s$) binding energy. v_R equals 3.70 mm/μs for $h\nu=2.1$ keV and 6.02 mm/μs for $h\nu=5.5$ keV, whereas the mean thermal velocity $\bar{v}_T$ at 300 K is 1.26 mm/μs. In Compton ionization for $h\nu\leq 5.5$ keV the energy transfer to the atom is much less than in photoabsorption [16], the kinetic energy of the ejected electron is small, and the ion recoil velocity is generally less than $\bar{v}_T$. The ratio R_m of the count rates for He^{2+} and He^+ is given by

$$R_m=\frac{\eta_p^{2+}\sigma_p^{2+}+\eta_C^{2+}\sigma_C^{2+}}{\eta_p^{+}\sigma_p^{+}+\eta_C^{+}\sigma_C^{+}}\ . \qquad (2)$$

The procedures used for calculating the efficiencies η_p^+, η_p^{2+}, η_C^+, and η_C^{2+}, and for extracting the experimental

TABLE I. Measured ratio R_m of the counting rates for He^{2+} and He^+ ions; and time-of-flight spectrometer collection efficiencies η for He^+ and He^{2+} ions created through photoabsorption (p) and Compton scattering (C). The last column lists $R'_m=(\eta_p^+/\eta_p^{2+})R_m$, Eq. (3).

$h\nu$ (keV)	R_m (%)	η_p^+	η_p^{2+}	η_C^+	η_C^{2+}	R'_m (%)
2.1	1.86±0.12	0.148	0.151	0.520	0.528	1.82
2.4	2.14±0.16	0.138	0.141	0.527	0.536	2.09
2.8	1.90±0.16	0.113	0.116	0.484	0.492	1.86
3.2	1.94±0.21	0.118	0.121	0.517	0.526	1.90
3.7	1.82±0.17	0.0961	0.0988	0.463	0.471	1.77
3.9	1.66±0.22	0.107	0.110	0.523	0.531	1.62
4.2	1.60±0.17	0.0902	0.0929	0.464	0.471	1.55
4.6	1.19±0.20	0.0982	0.101	0.519	0.528	1.15
5.0	1.44±0.19	0.0825	0.0851	0.461	0.469	1.40
5.5	1.15±0.25	0.0891	0.0922	0.508	0.516	1.11

count rates for He^{2+}, He^+, are discussed in the Appendix. Our experimental results for R_m are listed in Table I, along with the efficiencies. Note that the collection efficiency for Compton ions is between 3.5 and 5.7 times that for ions created by photoabsorption, implying that R_m weights preferentially the contribution of Compton ions. Although advantageous for observing the onset of Compton ionization, this fact has not been accounted for in previous comparisons [7,14,16,17] of our preliminary experimental results with calculations of the ratio R of the total double- and single-ionization cross sections [i.e., the right-hand side (RHS) of Eq. (2) with all $\eta=1$].

We also list in Table I the quantity

$$R'_m=\frac{\eta_p^+}{\eta_p^{2+}}R_m,$$

$$=\frac{\sigma_p^{2+}+\dfrac{\eta_C^{2+}}{\eta_p^{2+}}\sigma_C^{2+}}{\sigma_p^+ + \dfrac{\eta_C^+}{\eta_p^+}\sigma_C^+}. \tag{3}$$

R'_m reduces to $R_p=\sigma_p^{2+}/\sigma_p^+$ in the absence of Compton ionization. In Fig. 2 we plot $R'_m(h\nu)$, together with the MBPT results of Hino *et al.* [9] for $R_p(h\nu)$, and the $R_p(h\nu)$ obtained by Andersson and Burgdörfer [7] for two different models of final-state correlation. In one case the wave function is calculated with a full "Coulomb distortion factor" [Coulomb-distorted-wave (CDW) approximation]; in the other, corresponding to a "soft electron-electron collision" limit for the final state, only the linear term is retained in a high-energy expansion of $R_p(h\nu)$ in powers of $1/(h\nu)$ [$(h\nu)^{-1}$ approximation]. Differences between $R'_m(h\nu)$ and the calculated $R_p(h\nu)$ are attributable either to inaccuracies in the $R_p(h\nu)$ or to Compton ionization. At the bottom of Fig. 2 we show the ratio σ_C^+/σ_p^+ obtained with the cross sections of Andersson and Burgdörfer [7], Hino *et al.* [16], and Surić *et al.* [14]. Also shown for comparison is σ_C^+/σ_p^+ obtained with a simple free-electron model for Compton ionization described in the Appendix. For $h\nu<3$ keV σ_C^+/σ_p^+ is small, and the available calculations [7,14,16] indicate that σ_C^{2+} is negligible. Equation (3) then implies that Compton ionization causes $R'_m(h\nu)$ to be slightly smaller than $R_p(h\nu)$. One can estimate the difference using the calculated $\sigma_C^+(h\nu)/\sigma_p^+(h\nu)$. Andersson and Burgdörfer's cross sections imply a reduction of 1.0% at $h\nu=2.1$ keV, 2.4% at $h\nu=2.4$ keV, and 6.9% at $h\nu=2.8$ keV. Applying this correction to $R'_m(h\nu)$ for $h\nu=2.1$, 2.4, and 2.8 keV gives $R_p(2.1\text{ keV})=1.84\%$, $R_p(2.4\text{ keV})=2.14\%$, and $R_p(2.8\text{ keV})=1.99\%$. Using these three points plus $R_p(\infty)=1.66\%$ to fit the coefficients in the high-energy expansion [7] of $R_p(h\nu)$ in $(1/h\nu)$, retaining three terms, gives as our resulting estimate for $R_p(h\nu)$

$$R_p(h\nu)=0.0166+0.006\,44/(h\nu)+0.003\,17/(h\nu)^2 \tag{4}$$

(with $h\nu$ in keV); or $R_p(2.0\text{ keV})=2.06\%\pm0.15\%$, $R_p(2.5\text{ keV})=1.97\%\pm0.15\%$, where the uncertainties reflect the experimental statistical uncertainty. Equation (4) is also plotted in Fig. 2. If two terms are retained, an essentially identi-

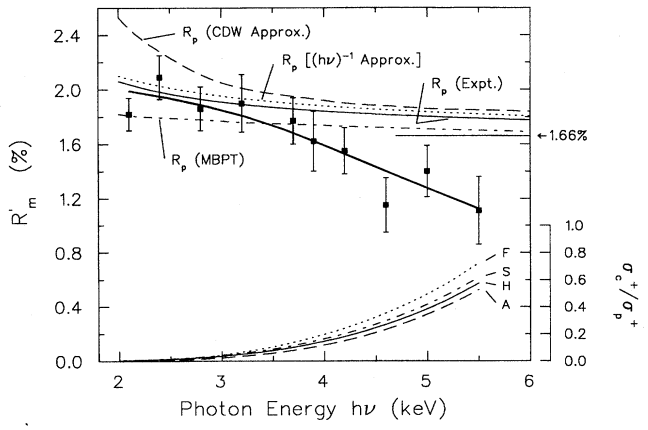

FIG. 2. Squares represent the experimental values of the double-to-single ionization ratio R'_m defined by Eq. (3). The heavy solid curve is a cubic spline fit to the data to guide the eye. Also shown are theoretical $R_p=\sigma_p^{2+}/\sigma_p^+$ of Andersson and Burgdörfer (upper dashed and dotted curves) and Hino *et al.* (upper dot-dashed curve). The curve labeled R_p (Expt.) represents an experimentally derived determination of R_p (see text). Bottom curves are calculations of σ_C^+/σ_p^+ by: A — Andersson and Burgdörfer, H — Hino *et al.*, S — Surić *et al.*, F — free-electron model.

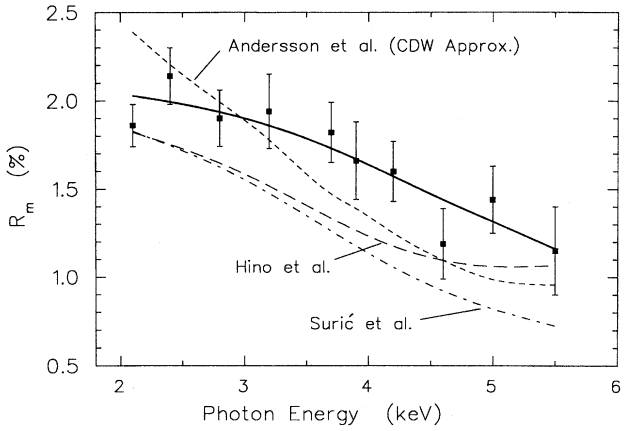

FIG. 3. Squares represent the measured values of the double-to-single ionization ratio R_m defined by Eq. (2). The solid curve is a cubic spline fit to the data. The remaining curves represent theoretical R_m obtained from Eq. (2) with the cross sections σ_p^+, σ_p^{2+}, σ_C^+, and σ_C^{2+} of Andersson and Burgdörfer (CDW approximation), Hino *et al.*, and Surić *et al.*

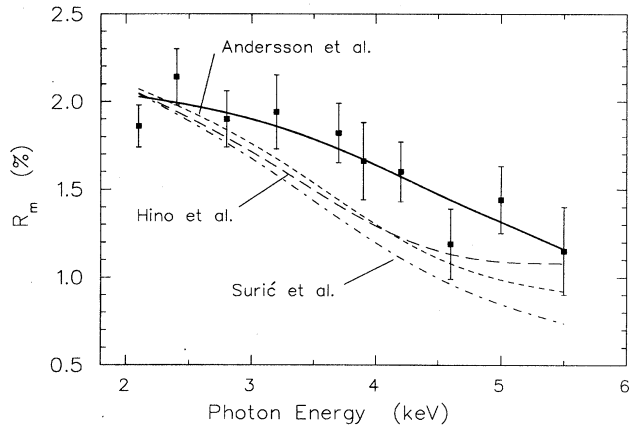

FIG. 4. As in Fig. 3, however the theoretical R_m were obtained with σ_p^{2+} from Eq. (4).

cal fit results with $R_p(h\nu)=0.0166+0.007\,68/(h\nu)$. Thus, the actual value of the $(h\nu)^{-2}$ coefficient (and higher-order coefficients) in the high-energy expansion cannot be accurately determined, and the $(h\nu)^{-1}$ coefficient is determined only crudely, given the experimental statistical uncertainty and the fact that the higher-order coefficients are not known. This estimate for R_p lies between the MBPT ($R_p=1.82\%$ at $h\nu=2.0$ keV, $\approx 1.79\%$ at 2.5 keV) and CDW ($R_p=2.53\%$, 2.25%, respectively) results, and is in good agreement with the $(h\nu)^{-1}$ approximation ($R_p=2.10\%$, 2.01%, respectively).

For $h\nu \gtrsim 4$ keV $R_m'(h\nu)$ falls off in a manner which is inconsistent with the calculated $R_p(h\nu)$, dropping well below the predicted high $h\nu$ limit of 1.66%. While in principle this could reflect inaccuracies in the $R_p(h\nu)$, we attribute it to the onset of single ionization from Compton scattering due to the clear correlation between the decrease in R_m' and the increase in σ_C^+/σ_p^+. This assignment also requires that $R_C=\sigma_C^{2+}/\sigma_C^+$ be well below 1.66% for $h\nu \leq 5.5$ keV [Eq. (3)]. Supporting this interpretation are the evident relative reliability [7] of the theoretical value for $R_p(\infty)$ and the fact that current calculations [7,14,16] all indicate that $R_C(h\nu) < 1\%$ for $h\nu \leq 5.5$ keV.

In Fig. 3 we compare our measured values of $R_m(h\nu)$ with the $R_m(h\nu)$ curves obtained from Eq. (2) with the cross sections σ_p^+, σ_p^{2+}, σ_C^+, and σ_C^{2+} of Hino *et al.* [9,16], Andersson and Burgdörfer (in the CDW approximation for σ_p^{2+}), and Surić *et al.* [14] (Surić *et al.* use the σ_p^+, σ_p^{2+} of Hino *et al.*) Andersson and Burgdörfer appear to overestimate, for $h\nu < 4$ keV or so, the rate of decrease in R_m; Hino *et al.* and Surić *et al.* less so. On the other hand, the calculations of Hino *et al.* and Surić *et al.* lie below experiment for $2.5 \lesssim h\nu \lesssim 4$ keV and $2.5 \lesssim h\nu \lesssim 5.5$ keV, respectively. One source of these disagreements, especially as $h\nu \to 2$ keV, lies with the calculated $\sigma_p^{2+}(h\nu)$. Substitution of the experimentally derived $\sigma_p^{2+}(h\nu)$ from Eq. (4), however, permits an examination of the discrepancies between the experimental and calculated R_m which originate solely with the calculated values of the Compton ionization cross sections σ_C^+ and σ_C^{2+}. The results are shown in Fig. 4. [Similar results are obtained with the $(h\nu)^{-1}$ approximation for R_p.] All of the calculated curves now exhibit very similar behavior for $h\nu < 4.5$ keV, and all overestimate the rate of decrease in R_m. This implies that, in some combination, the calculated ratio σ_C^+/σ_p^+ (cf. Fig. 2) increases too rapidly with $h\nu$ in this energy range or the calculated ratio $R_C=\sigma_C^{2+}/\sigma_C^+$ is too small. The predicted values for R_C at $h\nu=3.9$ keV from Refs. [7], [14], and [16] are approximately 0.24%, 0.30%, and 0.41%, respectively. Experimental measurements of the individual cross-section ratios σ_C^{2+}/σ_C^+ and σ_C^+/σ_p^+ are clearly desirable in order to clarify this issue. The calculations begin to converge with experiment again for $h\nu \gtrsim 4.5$ keV, more so in the case of Hino *et al.*, less so in the case of Surić *et al.*

Finally, we comment on the consistency of our measurements with those of Levin *et al.*, who quote [10,11]: $R(2.05\ \text{keV})=1.99\%\pm0.22\%$, $R(2.4\ \text{keV})=1.96\%\pm0.18\%$, $R(2.8\ \text{keV})=1.60\%\pm0.30\%$, $R(3.3\ \text{keV})=1.73\%\pm0.19\%$, and $R(4.0\ \text{keV})=1.76\%\pm0.33\%$. $R(h\nu)$ cannot be *directly* compared with $R_m(h\nu)$; however, because R_m and R_m' preferentially weight Compton ionization one should have $R_m'(h\nu) < R(h\nu) < R_p(h\nu)$, i.e., $R(h\nu)$ should lie between the experimental R_m' curve and the curve labeled R_p (Expt.) in Fig. 2. For $h\nu=2.05$, 2.4, and 4.0 keV, the quoted value of R is in excellent agreement with the "expected" value based on this argument. For $h\nu=3.3$ keV the expected value lies within the experimental error bar, while for $h\nu=2.8$ keV the expected value lies near the top of the experimental error bar. Thus, there is good overall consistency, given the stated statistical uncertainties.

In conclusion, we have measured the effect of Compton scattering on the double-to-single ionization ratio in He for $2.1 \leq h\nu \leq 5.5$ keV. We emphasize that the comparison of our experimental results with calculated cross sections must occur through Eq. (2), using the efficiencies η and experimental values of R_m listed in Table I.

Note added in proof. Recently, Spielberger *et al.* [Phys. Rev. Lett. **74**, 4615 (1995)] have reported measurements of

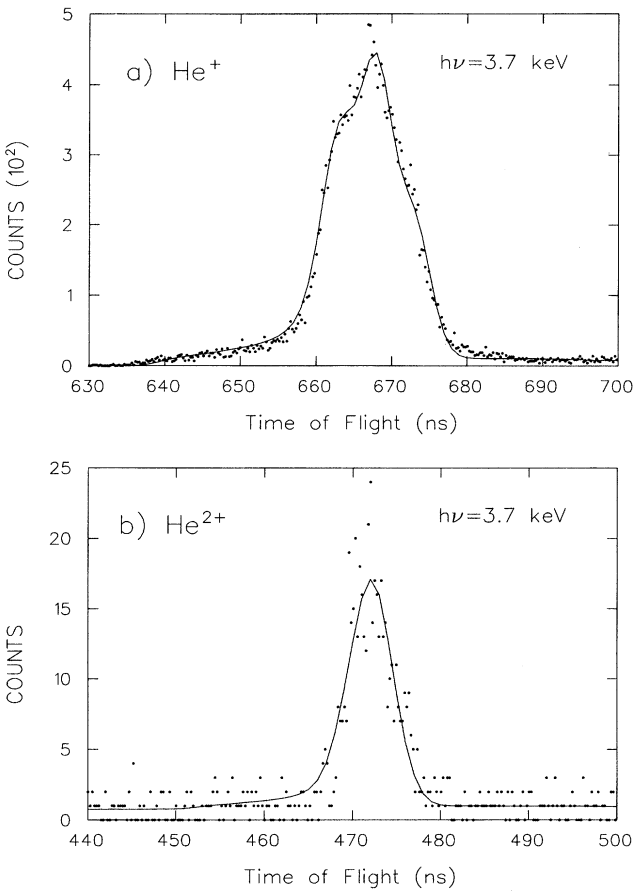

FIG. 5. (a) Dots represent the experimental time-of-flight spectrum for He^+ for $h\nu=3.7$ keV. The solid curve is the time-resolved efficiency curve. (b) same as (a), for He^{2+}.

R_p and R_C in He with broadband radiation near $h\nu=7.0$ and 8.8 keV, respectively.

This work was supported by the U.S. Department of Energy through Los Alamos National Laboratory and by the National Science Foundation under Grant No. PHY-9317934. We acknowledge helpful discussions with P. Bergstrom, J. Burgdörfer, K. Hino, and T. Surić.

APPENDIX A

Let $\eta_{\rm tot}$ denote the overall probability that an ion which is created along the photon beam path in the extraction region of the TOFS (Fig. 1) will reach the MCP detector, irrespective of its arrival time. (In the present discussion we suppress superscripts $+,2+$ and subscripts p,C.) $\eta_{\rm tot}$ is given by the following integral over the phase space of the parameters describing ion creation

$$\eta_{\rm tot}=\int_0^T dt\int_{-y_0}^{y_0} dy\int_{\Delta z} dz\int_{\Delta x} dx\int d^3v_T\int d^3v_R \times P(t,x,y,z,\vec{v}_T,\vec{v}_R)N(t,x,y,z,\vec{v}_T,\vec{v}_R), \quad \text{(A1)}$$

where t is the time the ion is created ($t=0$ represents the trailing edge of the preceding field pulse), x and z define the initial position of the ion transverse to the photon beam (Fig. 1; Δx and Δz represent the transverse beam widths), y is the initial position of the ion along the photon beam direction ($2y_0$ is the length of the extraction region), $\vec{v}_T$ is the thermal velocity of the ion, $\vec{v}_R$ is the recoil velocity, $P(t,x,y,z,\vec{v}_T,\vec{v}_R)$ is the probability density that the ion is created at t, x, y, z with velocities $\vec{v}_T$ and $\vec{v}_R$, and $N(t,x,y,z,\vec{v}_T,\vec{v}_R)$ equals 1 if the ion reaches the detector and 0 otherwise. P is assumed to be uniform in x, y, z, and t. The v_T dependence is given by the Maxwell velocity distribution. For single ionization from photoabsorption the dependence of v_R on the electron emission direction (arising from the photon momentum) is weak, and we adopt a constant v_R given by Eq. (1), which is an excellent approximation to the mean. Because the electric field is polarized along the TOFS (z) axis, the angular distribution of recoil velocities is $\cos^2\theta$ about z. In double ionization from photoabsorption for $h\nu>2$ keV, the photon energy is transferred predominantly to the primary photoelectron [9], in which case v_R is again given to a good approximation by Eq. (1). Also, we assume that the angular distribution of recoil velocities is again $\cos^2\theta$.

In Compton single ionization from He, v_R can depend strongly on the electron emission direction and Compton scattering angle. Because v_R is small, however, it is adequate to adopt a constant value equal to the mean ion recoil velocity $\bar{v}_R$. To estimate $\bar{v}_R$ as a function of the incident photon energy $h\nu$, we first note that for given Compton scattering angle θ, energy $h\nu'$ of the scattered photon, and electron emission direction $\Omega_e=\theta_e,\phi_e$, the four kinematic constraints of energy and momentum conservation determine the magnitude v_e of the electron emission velocity, and both the magnitude v_R and direction $\Omega_R=\theta_R,\phi_R$ of the ion recoil velocity. Thus, $\vec{v}_R=\vec{v}_R(\theta,h\nu',\Omega_e)$. We make the approximation that, for given θ, $h\nu'$ assumes only the fixed value associated with free-electron Compton scattering, i.e., $h\nu'=h\nu-(1-\cos\theta)/m_0c^2$, where m_0 is the electron rest mass; thus neglecting, for example, the Doppler broadening of the scattered photon energy associated with the finite momentum distribution of the He($1s$) electron. Next, we consider an isotropic angular distribution for the Compton electron, thereby neglecting the dependence of the cross section on the electron emission direction, and define $\bar{v}_R(\theta,h\nu')$ as the resulting average of $v_R(\theta,h\nu',\Omega_e)$ over Ω_e. Lastly, we average $\bar{v}_R(\theta,h\nu')$ with respect to the photon scattering direction θ,ϕ by weighting $\bar{v}_R(\theta,h\nu')$ with the Klein-Nishina differential cross section for Compton scattering from a free electron [20], taking as a minimum scattering angle θ_b the scattering angle at which the energy transfer $\Delta E=h\nu-h\nu'$ to a free electron equals the He($1s$) binding energy, 24.59 eV. The mean ion recoil velocity $\bar{v}_R$ then becomes, for $h\nu'\approx h\nu$,

$$\bar{v}_R=\frac{\int_{\theta_b}^{\pi}d\theta\int d\Omega_e\,\sin\theta(2-\sin^2\theta)v_R(\theta,h\nu',\Omega_e)}{4\pi\int_{\theta_b}^{\pi}d\theta\,\sin\theta(2-\sin^2\theta)}. \quad \text{(A2)}$$

$\bar{v}_R$ ranges from 0.45 mm/μs for $h\nu=2.8$ keV to 0.84 mm/μs for $h\nu=5.5$ keV. We note that integrating the Klein-Nishina cross section over scattering directions satisfying $\theta_b \leq \theta \leq \pi$, and multiplying by 2, gives a "free-electron" approximation for the total Compton single ionization cross section for He

$$\sigma_C^+(h\nu)=0.75\sigma_T[1+\cos\theta_b+(1+\cos^3\theta_b)/3], \quad \text{(A3)}$$

where σ_T is the Thomson cross section, 0.665 barns.

We next define a time-resolved efficiency $\eta(t_{\rm tf})$ such that $\eta(t_{\rm tf})dt_{\rm tf}$ is the probability that an ion will reach the detector with a time of flight between $t_{\rm tf}$ and $t_{\rm tf}+dt_{\rm tf}$. We have

$$\eta_{\rm tot}=\int_0^\infty dt_{\rm tf}\eta(t_{\rm tf}), \quad \text{(A4)}$$

where $t_{\rm tf}=0$ represents the leading edge of the field pulse. For each photon energy at which $R_m(h\nu)$ was measured, time resolved efficiencies $\eta_p^+(t_{\rm tf})$, $\eta_C^+(t_{\rm tf})$, $\eta_p^{2+}(t_{\rm tf})$, and $\eta_C^{2+}(t_{\rm tf})$ were computed using a Monte Carlo procedure. The weighted sum $\sigma_C^+\eta_C^+(t_{\rm tf})+\sigma_p^+\eta_p^+(t_{\rm tf})$ should simply reproduce the experimental time-of-flight spectrum for He^+ (and similarly for He^{2+}), and so the efficiency curves for He^+ and He^{2+} were fit to the corresponding time-of-flight spectra in a least-squares calculation, using as parameters the cross-section ratio σ_C^+/σ_p^+ (or $\sigma_C^{2+}/\sigma_p^{2+}$), a constant background, and an overall time shift of the experimental spectrum. Small adjustments were made in experimental parameters such as the precise position of the synchrotron beam between TOFS plates P_1 and P_2, the beam width, etc., so as to optimize the fit. Figure 5(a) shows the results for He^+ for $h\nu=3.7$ keV. Very good agreement is obtained. The shoulders at 663 and 673 ns represent photoabsorption ions with recoil velocities directed toward and away from the detector, respectively. The broad shoulder extending up to 637 ns is from ions which drift close to plate P_2 before the field pulse arrives. The tail beyond 680 ns represents the late arrivals. Because the tail decreases asymptotically it is necessary to introduce a cutoff, which we take at 700 ns. We therefore now define the time-independent efficiencies η_p^+ and η_C^+ appearing in Eq. (2) as the integrals over time of $\eta_p^+(t_{\rm tf})$ and $\eta_C^+(t_{\rm tf})$, respectively, for $630\leq t_{\rm tf}\leq 700$ ns. [$\eta_p^+(t_{\rm tf})$, $\eta_C^+(t_{\rm tf})=0$ for $t_{\rm tf}<630$ ns.] Similarly, the number of He^+ counts in the experimental peak is taken to be the total counts for $630\leq t_{\rm tf}\leq 700$ ns minus the background counts. Figure 5(b) shows the results for He^{2+}. For He^{2+} the experimental count rate and the efficiencies η_p^{2+}, η_C^{2+} pertain to the interval $445\leq t_{\rm tf}\leq 490$ ns.

The sensitivity of the efficiencies to various experimental parameters, such as those mentioned above, was studied. Note from Eq. (2) that R_m can be considered a function of the efficiency *ratios* η_p^{2+}/η_p^+, η_C^+/η_p^+, and η_C^{2+}/η_p^+. Our estimated uncertainties in the calculated values of these ratios are $\pm 1\%$ for η_p^{2+}/η_p^+ (similarly for η_C^{2+}/η_C^+), and $\pm 10\%$ for η_C^+/η_p^+ and η_C^{2+}/η_p^+.

[1] M. Tinkham, *Group Theory and Quantum Mechanics* (McGraw-Hill, New York, 1964).

[2] F. W. Byron and C. J. Joachain, Phys. Rev. **164**, 1 (1967).

[3] T. Åberg, Phys. Rev. A **2**, 1726 (1970).

[4] R. L. Brown and R. J. Gould, Phys. Rev. D **1**, 2252 (1970).

[5] M. Ya Amusia, E. G. Drukarev, V. G. Gorshkov, and M. P. Kazachkov, J. Phys. B **8**, 1248 (1975).

[6] A. Dalgarno and H. R. Sadeghpour, Phys. Rev. A **46**, R3591 (1992).

[7] L. R. Andersson and J. Burgdörfer, Phys. Rev. Lett. **71**, 50 (1993), and private communication.

[8] T. Ishihara, K. Hino, and J. H. McGuire, Phys Rev. A **44**, R6980 (1991).

[9] K. Hino, T. Ishihara, F. Shimizu, N. Toshima, and J. H. McGuire, Phys. Rev. A **48**, 1271 (1993).

[10] J. C. Levin, D. W. Lindle, N. Keller, R. D. Miller, Y. Azuma, N. Berrah Mansour, H. G. Berry, and I. A. Sellin, Phys. Rev. Lett. **67**, 968 (1991).

[11] J. C. Levin, I. A. Sellin, B. M. Johnson, D. W. Lindle, R. D. Miller, N. Berrah Mansour, Y. Azuma, H. G. Berry, and D. H. Lee, Phys. Rev. A **47**, R16 (1993).

[12] J. A. R. Samson, C. H. Greene, and R. J. Bartlett, Phys. Rev. Lett. **71**, 201 (1993).

[13] J. A. R. Samson, Z. X. He, R. J. Bartlett, and M. Sagurton, Phys. Rev. Lett. **72**, 3329 (1994).

[14] T. Surić, K. Pisk, B. A. Logan, and R. H. Pratt, Phys. Rev. Lett. **73**, 790 (1994), and private communication.

[15] L. Andersson and J. Burgdörfer, Phys. Rev. A **50**, R2810 (1994).

[16] K. Hino, P. M. Bergstrom, and J. H. Macek, Phys. Rev. Lett. **72**, 1620 (1994), and private communication.

[17] P. M. Bergstrom, K. Hino, and J. H. Macek, Phys. Rev. A **51**, 3044 (1995).

[18] P. Eisenberger and P. M. Platzmann, Phys. Rev. A **2**, 415 (1970).

[19] P. M. Bergstrom, T. Surić, K. Pisk, and R. H. Pratt, Phys. Rev. A **48**, 1134 (1993), and references therein.

[20] O. Klein and Y. Nishina, Z. Phys. **52**, 853 (1929).